

Limitations of coupled cluster approximations for highly accurate investigations of Rb_2^+

Jan Schnabel,¹ Lan Cheng,² and Andreas Köhn¹

¹*Institute for Theoretical Chemistry and Center for Integrated Quantum Science and Technology, University of Stuttgart, 70569 Stuttgart, Germany*

²*Department of Chemistry, The Johns Hopkins University, Baltimore, Maryland 21218, United States*

(*Electronic mail: schnabel@theochem.uni-stuttgart.de)

(*Electronic mail: lcheng24@jhu.edu)

(*Electronic mail: koehn@theochem.uni-stuttgart.de)

(Dated: July 2, 2021)

We reveal limitations of several standard coupled-cluster (CC) methods with perturbation-theory based noniterative or approximate iterative treatments of triple excitations when applied to the determination of highly accurate potential energy curves (PECs) of ionic dimers, such as the $X^2\Sigma_g^+$ electronic ground state of Rb_2^+ . Such computations are of current interest for the understanding of ion-atom interactions in the ultracold regime. We demonstrate that these coupled-cluster methods lead to an unphysical long-range barrier for the Rb_2^+ system. The barrier is small but clearly spoils the entire long-range behavior of the PEC. The effect is also found for other X_2^+ systems, like $X = \text{Li}, \text{Na},$ and K . Calculations using a new flexible framework for obtaining leading perturbative triples corrections derived using an analytic CC singles and doubles (CCSD) energy derivative formulation demonstrate that the origin of this problem lies in the use of \hat{T}_3 amplitudes obtained from approximate CC singles, doubles and triples (CCSDT) amplitude equations. It is shown that the unphysical barrier is related to a symmetry instability of the underlying Hartree-Fock mean-field solution. Physically meaningful perturbative corrections in the long-range tail of the PEC may instead be obtained using symmetry-broken reference determinants.

I. INTRODUCTION

The understanding and the gain of control of interacting neutral atoms in the ultracold quantum regime has grown substantially over the past decades. The achievements, to mention only a few of them, reach from Bose-Einstein condensation (BEC)¹, over Rydberg systems²⁻⁴ to creating and controlling ultracold molecules⁵⁻⁷. While for neutral atoms reaching the ultracold quantum scattering regime (i.e. s-wave collision regime) is nowadays well established, it is still a non-trivial challenge to reach the quantum scattering regime for hybrid ion-atom systems due to more stringent temperature requirements⁸. This is extremely desirable as hybrid ion-atom systems are expected to pave the way for novel experiments, phenomena and applications – among others the precision measurements of ion-atom collision parameters and associated molecular potentials⁹⁻¹¹.

Novel experimental approaches have been proposed recently in Refs. 12,13. Here the ion-atom interaction for a core of a giant Rydberg atom immersed in a BEC of ^{87}Rb leading to a temperature environment below a microkelvin has been studied. In principle, the experimental accuracy achievable with this approach is in the MHz ($= \mathcal{O}(10^{-5} \text{ cm}^{-1})$) domain with a characteristic range of the ion-atom interaction (for Rb) of $R^* = \sqrt{\mu C_4} \approx 5000 a_0$ ⁸.

These pilot experiments, see e.g. Ref. 12 and references therein, aim at entering the s-wave scattering regime and eventually studying the ro-vibrational structure (of, e.g., the threshold bound states) and charge-transfer processes of Rb_2^+ . Therefore, highly accurate potential energy curves (PECs) are needed as a starting point for subsequent studies of corresponding properties related to design and performance of these experiments. The PECs have to be accurate not only in the long-range region (up to

$R_\infty = R^* \approx 5000 a_0$ to investigate scattering effects sufficiently), but also in the short-range region (to provide an accurate insight into the ro-vibrational structure). The long-range part of the interaction potential between an S-state ion and an S-state atom in the electronic ground state is given by⁸

$$V_{\text{ion-atom}}^{\text{LR}} \approx -\frac{C_4^{\text{ind}}}{R^4} - \frac{C_6^{\text{ind}}}{R^6} - \frac{C_6^{\text{disp}}}{R^6} + \dots \quad (1)$$

The C_4^{ind} and C_6^{ind} terms describe the interaction between the charge of the ion and the induced electric dipole (quadrupole) moment of the atom, while the C_6^{disp} dispersion term represents the interaction between instantaneous dipole-induced dipole moments of the ion and atom arising due to quantum fluctuations⁸. Patil and Tang approximately evaluated multipolar polarizabilities and dispersion coefficients of homonuclear and heteronuclear interactions of both alkali and alkaline earth atoms and ions, respectively in Ref. 14. This can be further used for models studying reactive collisions, cf. e.g. Refs. 15,16. However, using approximate values for the dispersion coefficient might turn out to be insufficient for predictions to guide novel experiments. It is thus of significant interest to obtain accurate PECs using *ab-initio* calculations.

Theoretical investigations of X_2^+ -systems (with $X = \text{Li, Na, K, Rb}$)^{17–20} have been reported earlier. As perhaps the only example aiming at high accuracy, Tomza *et al.* reported a scheme for obtaining a PEC of Li_2^+ from relativistic coupled cluster (CC) calculations.¹¹ Our efforts originally aimed at a first high accuracy calculation of PECs for homonuclear molecular ions containing heavier alkali metal species using an additivity scheme as laid out in Section II. Our calculations revealed some non-trivial subtleties in CC methods with noniterative and approximate iterative treatment of triple excitations including the coupled-cluster singles and doubles augmented with a noniterative triples correction [CCSD(T)] method, – the ‘gold standard’ of quantum chemistry. The corresponding theoretical basics are outlined in Sec. III. As shown in Sec. IV, this problem leads to an unphysical barrier in the long-range region of the PEC. The present paper thus is focused on understanding and solving this problem. In Sec. V the problem is analyzed and

attributed to a dominant contribution of the Fockian in the corresponding equations of these approximate treatments of triple excitations. We show that physically meaningful perturbative corrections in the long-range can be obtained using symmetry-broken reference determinants. Moreover, we present an alternative approach with approximate treatment of triple excitations to obtain high accuracy and simultaneously avoiding the long-range problem to extract valuable properties such as dispersion coefficients. Finally, Section VI gives a summary and an outlook.

II. COMPUTATIONAL ASPECTS

High-accuracy quantum-chemical calculations of atomic and molecular energies often rely on additivity schemes.^{21–26} The present study was originally designed to follow the HEAT (High accuracy Extrapolated Ab initio Thermochemistry)^{24,27} protocol to obtain as accurate energies as the present computational resources allow in a systematic way. Here we assume that the total electronic energy E of a given molecular system can be calculated using the following additivity scheme

$$E = E_{\text{HF}}^\infty + \Delta E_{\text{CCSD(T)}}^\infty + \Delta E_{\text{HLC}} + \Delta E_{\text{higher-rel}}, \quad (2)$$

in which E_{HF}^∞ and $\Delta E_{\text{CCSD(T)}}^\infty$ are the estimated complete basis-set (CBS) limit values for the Hartree-Fock (HF) energy and the CCSD(T) correlation energy, and E_{HLC} represents the high-level correlation (HLC) contribution [those beyond CCSD(T)]. E_{HF}^∞ , $\Delta E_{\text{CCSD(T)}}^\infty$, and E_{HLC} can be obtained from HF and CC calculations either using the small-core effective core potential (scECP) ECP28MDF from Ref.²⁸, where the $4s^2 4p^6 5s^1$ electrons of Rb are treated explicitly and all the others are modelled via a scalar-relativistic pseudopotential (PP), or using the all-electron spin-free exact two-component theory in its one-electron variant (SFX2C-1e)^{29,30} to treat scalar-relativistic effects. We can use spin-unrestricted (UHF) or spin-restricted open-shell (ROHF) approaches for the HF part of Eq. (2) and for generating the orbitals for the subsequent single-reference CC calculations. For the latter we used an unrestricted spin-orbital formalism in its sin-

gles and doubles variant augmented with a noniterative triples method based on a ROHF reference – the ROHF-CCSD(T) method^{31–34} [also often referred to as ‘RHF-UCCSD(T)’]. The HLC contributions include the full triples correction obtained as the difference between full CC singles doubles and triples (CCSDT)^{35,36} and CCSD(T) results using smaller basis sets and the quadruples correction obtained as the difference between CC singles doubles triples augmented with noniterative quadruples [CCSDT(Q)]^{37,38} and CCSDT results (with, in general, even smaller basis sets). Here we used the CCSDT(Q)/B variant for ROHF reference³⁹.

The overall goal of obtaining highly accurate ground-state PECs for Rb_2^+ requires using large basis sets, which are flexible enough to describe both the long-range part and the repulsive part as accurately as possible. Moreover, the basis set should show smooth convergence behaviour when extrapolating the results to estimate the CBS limit. Recently, correlation-consistent Gaussian basis sets for use in correlated molecular calculations have been published for alkali metal elements in Ref.⁴⁰. Those basis sets [aug-cc-p(w)CVnZ-PP] are designed for the ECP28MDF pseudopotential and are available up to quintuple- ζ quality.

These methods define the theoretical framework for the present study. However, when proceeding to obtain the CCSD(T) part of the PECs for Rb_2^+ , a supposedly spurious hump in the long-range potential was observed. Therefore, no further effort was put into the calculation of the $\Delta E_{\text{higher-rel}}$ part of Eq. (2). Instead, our attention is placed on investigating the origin of this problem in the CCSD(T) potential energy surface, for what we have also carried out calculations of the Rb_2^+ PEC using approximate iterative triples methods including CCSDT-n ($n=1b, 2, 3$, and 4)^{41,42} as well as CCSDT and CCSDT(Q)^{37–39} calculations. Symmetry-broken ROHF-CCSD(T) calculations allowing for charge localization on one Rb atom have been carried out as well.

The ECP-based ROHF-CCSD(T) calculations described above have been performed using the MOLPRO 2018.2 program package^{43–47}, the SFX2C-1e-ROHF-CCSD(T), all CCSD(T) _{Λ} ,^{48–50} CCSDT, and CCSDT-n ($n=1b, 2, 3$, and 4) calculations have been carried out using the CFOUR program package^{34,51–53}, and all CCSDT(Q) energies were com-

puted using the MRCC program suite^{38,54,55}.

III. THEORY

Coupled-cluster theory is based on a similarity transformation of the Hamiltonian and a projective solution of the resulting stationary Schrödinger equation. This leads to the equations

$$E = \langle \Phi_0 | \bar{H} | \Phi_0 \rangle \quad (3a)$$

$$0 = \langle \Phi_I | \bar{H} | \Phi_0 \rangle, \quad (3b)$$

where

$$\bar{H} = e^{-\hat{T}} \hat{H} e^{\hat{T}} \quad (4)$$

is the similarity transformed electronic clamped-nuclei Hamiltonian and $|\Phi_0\rangle$ the reference wavefunction. The excited determinants $|\Phi_I\rangle$ are chosen to match the excitations reached by the cluster operator $\hat{T} = \sum_n \hat{T}_n$, which consists of n -fold excitation operators defined via

$$\hat{T}_n = \frac{1}{(n!)^2} \sum_{ijk, \dots abc, \dots} [T_n]_{ijk, \dots}^{abc, \dots} \hat{a}_a^\dagger \hat{a}_b^\dagger \hat{a}_c^\dagger \dots \hat{a}_k \hat{a}_j \hat{a}_i \dots \quad (5)$$

Here, the symbols \hat{a}^\dagger are creation and the \hat{a} annihilation operators, $[T_n]_{ijk, \dots}^{abc, \dots}$ are the cluster amplitudes and the indices a, b, c, \dots run over virtual and i, j, k, \dots over occupied orbitals, respectively. The electronic Hamiltonian \hat{H} is usually formulated as

$$\hat{H} = E_0 + \hat{f}_N + \hat{W}_N \quad (6a)$$

$$= E_0 + \sum_{pq} f_p^q \hat{a}_p^\dagger \hat{a}_q + \frac{1}{4} \sum_{pqrs} g_{pr}^{qs} \hat{a}_p^\dagger \hat{a}_r^\dagger \hat{a}_s \hat{a}_q, \quad (6b)$$

with the one-particle operator \hat{f}_N containing the Fock matrix f_p^q and the two-particle operator \hat{W}_N with the anti-symmetrized two-electron integrals g_{pr}^{qs} . For later reference, we note that the coupled-cluster equations, Eqs. (3), can be summarized as an energy functional⁵⁶

$$\mathcal{L} = \langle \Phi_0 | (1 + \hat{\Lambda}) \bar{H} | \Phi_0 \rangle \quad (7)$$

where the Lambda operator was introduced, consisting of a set of deexcitation operators with analogous

definition to that of the excitation operators of the cluster operator.

For CCSD, the cluster operator is truncated after double excitations, but it is well-known that quantitative computations require at least an approximate account of triple excitations. In order to cut down the computational expense of full CCSDT computations, it is usual to approximate the triple excitations perturbatively. One of the first approaches implemented is the CCSD[T] energy correction [originally called CCSD+T(CCSD)]⁵⁷, which is based on a fourth-order perturbation theory contribution and is given, assuming canonical (Hartree-Fock) orbitals, in terms of

$$\begin{aligned}\Delta E^{[T]} &= \Delta E^{(4)} = -\langle \Phi_0 | \hat{T}_3^\dagger \hat{f}_N \hat{T}_3 | \Phi_0 \rangle \\ &= -\frac{1}{36} \sum_{ijk} \sum_{abc} \left([T_3]_{ijk}^{abc} \right)^2 \cdot D_{ijk}^{abc},\end{aligned}\quad (8)$$

with \hat{T}_3 defined via Eq. (5) and D_{ijk}^{abc} expressed in terms of orbital energies ε_p via

$$D_{ijk}^{abc} = \varepsilon_a + \varepsilon_b + \varepsilon_c - \varepsilon_i - \varepsilon_j - \varepsilon_k \quad (9)$$

The triples amplitudes are computed from the converged CCSD amplitudes

$$[T_3]_{ijk}^{abc} = \frac{-\langle \Phi_{ijk}^{abc} | [\hat{W}_N, \hat{T}_{2, \text{CCSD}}] | \Phi_0 \rangle}{\varepsilon_a + \varepsilon_b + \varepsilon_c - \varepsilon_i - \varepsilon_j - \varepsilon_k}, \quad (10)$$

where Φ_{ijk}^{abc} denotes a triply excited determinant. By considering an additional term including CCSD singles excitations one obtains an energy correction, which is formally of fifth-order in the perturbation expansion, yielding

$$\begin{aligned}\Delta E^{(5)} &= \left\langle \Phi_0 \left| \hat{T}_1^\dagger \hat{W}_N \hat{T}_3 \right| \Phi_0 \right\rangle \\ &= \frac{1}{4} \sum_{ijk} \sum_{abc} [T_1]_i^a \langle bc || jk \rangle [T_3]_{ijk}^{abc}.\end{aligned}\quad (11)$$

The well-known CCSD(T) method^{31,34} includes this fifth-order term:

$$\Delta E^{(T)} = \Delta E^{(4)} + \Delta E^{(5)} = \Delta E^{[T]} + \Delta E^{(5)}. \quad (12)$$

The fifth-order term can be understood in terms of an alternative definition of the unperturbed system⁴⁸

and was shown to be often essential for a good performance of the perturbative triples correction.⁵⁸

In addition, a number of further approximations to CCSDT exist, which treat the triple excitations perturbatively, but include them self-consistently into the solution of the coupled-cluster equations. This is in particular the class of CCSDT- n methods of which we in this work consider the variants $n = 1b, 2, 3,$ and 4 .⁵⁹⁻⁶² CCSDT-1b can be largely viewed as the self-consistent version of CCSD(T), as it includes the same leading-order terms in the coupled-cluster equations, which also lead to the perturbative energy expression, Eq. (12). In addition, it includes contributions of $\hat{T}_1 \hat{T}_3$ to the doubles residual, which is thus complete (compared to the doubles residual of the full CCSDT method). The other methods, CCSDT-2 and CCSDT-3, subsequently include further terms in the residual for the triple excitations, while avoiding any N^8 -scaling contributions. Hence, up to this point the only contribution of the cluster operator \hat{T}_3 in the triple excitation residual appears via $\langle \Phi_{I_3} | \hat{f}_N \hat{T}_3 | \Phi_0 \rangle$ defining an equation for determining the corresponding \hat{T}_3 amplitudes independent of \hat{T}_3 itself. These amplitudes are calculated ‘on the fly’ immediately followed by calculating the resulting contribution of \hat{T}_3 in the projection onto the singles and doubles subspaces. These computational savings are lost when proceeding to CCSDT-4 which partially includes N^8 terms. This method goes beyond the perturbative approximation of \hat{T}_3 and includes the full term $\langle \Phi_{I_3} | [\hat{H}, \hat{T}_3] | \Phi_0 \rangle$. While the CCSDT- n methods do not find wide use for the computation of ground state energies, they provide a useful hierarchy to investigate any short-comings of CCSD(T).

IV. RESULTS

In this work we concentrate on the ROHF-CCSD(T) part of Eq. (2) for the calculation of the $X^2\Sigma_g^+$ ground state of Rb_2^+ . There is a second state of ungerade symmetry (i.e. $(1)^2\Sigma_u^+$) which becomes degenerate to the former one in the long-range region, as shown in Fig. 1. However, in the following we will solely focus on the long-range region of the $X^2\Sigma_g^+$ PEC.

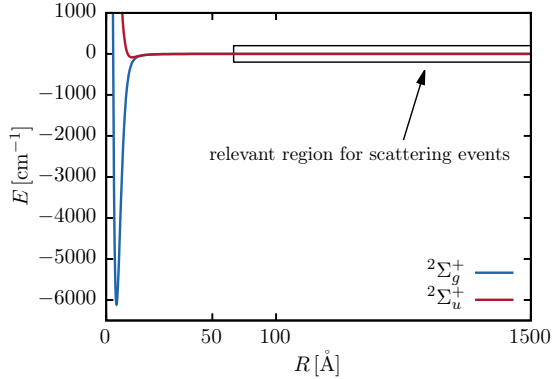


Figure 1. Schematic illustration of complete potential energy curves (PECs) of the Rb_2^+ ground states $^2\Sigma_g^+$ and $^2\Sigma_u^+$. For studying the ion-atom interaction we need high accuracy over the whole range of the PEC to obtain both the rovibrational structure and the long-range region, relevant for investigating scattering events, highly accurate.

A. Breakdown of CCSD(T)

In all calculations, we tightened the convergence thresholds for both the underlying ROHF calculations and the subsequent coupled-cluster part as much as possible to avoid numerical errors. Figure 2 gives an overview of the resulting long-range parts of the corresponding PECs for the aug-cc-pCVnZ-PP basis sets ($n = \text{T, Q, 5}$). The curves for the ROHF reference and the CCSD energies show the expected long-range behavior, i.e. a weakly attractive potential that decays in accordance with Eq. (1). However, including perturbative triples corrections via CCSD(T) produces a small but clearly unexpected barrier in the long-range region at $R \approx 100 \text{ \AA}$ with a magnitude of $\approx 0.15 \text{ cm}^{-1}$ above the dissociation asymptote. The triples corrections included via [T] are correct to fourth order perturbation theory and produce a slightly more pronounced barrier at the same position. This indicates that the additional fifth-order terms included in the (T) correction serve for a slight, but certainly not sufficient, compensation. This will be discussed in more detail in Sec. V.

To the best of our knowledge this kind of unphysical behavior seems to be undocumented so far. It appears to be an inherent problem for the CCSD(T) method, since other sources of error can be excluded

after thoroughly investigating their impact (see also supplementary material):

- (i) numerical errors due to convergence issues: We used tightened thresholds a priori, with numerical noise for energies in the order of $< \mathcal{O}(2.5 \cdot 10^{-7} \text{ cm}^{-1})$.
- (ii) insufficient basis set: As seen in Fig. 2, the shape of the PEC for ROHF-CCSD does not depend on the basis set and the height of the spurious barrier at the ROHF-CCSD(T) level even increases for larger basis sets. This also implies that basis set superposition is not a cause of the problem either, which we could also confirm by applying the counterpoise correction scheme to account for basis set superposition errors.
- (iii) the choice of reference wavefunction: We computed the long-range tail of the PECs using UHF references with the CFOR program and obtained virtually the same result, with absolute energy differences $\mathcal{O}(10^{-2} \text{ cm}^{-1})$.
- (iv) use of spin-unrestricted or partially spin-restricted coupled cluster theory [i.e. RHF-UCCSD(T) or RHF-RCCSD(T)], see, e.g., Refs. 45–47: This only leads to energy differences in the long-range region in the order of $\mathcal{O}(10^{-4} \text{ cm}^{-1})$

We also found that this unphysical barrier is universal for X_2^+ systems ($\text{X} = \text{Li, Na, K, Rb, Cs}$), which is shown in the supplementary material. Moreover, it is not an artefact due to the approximative nature of the scECP treatment since an all-electron SFX2C-1e-ROHF-CCSD(T) calculation at aug-cc-pwCVTZ-X2C level of theory leads to the long-range behavior shown in Fig. 3. Obviously, the long-range barrier is still present, at the same position with the same order of magnitude. Finally, we note that there are no multireference effects expected for the Rb_2^+ system. The two near-degenerate states ($X^2\Sigma_g^+$ and $(1)^2\Sigma_u^+$) are of different symmetry and thus do not mix. This is in contrast to what has been reported, e.g., in Ref. 63 for the ground state PEC of neutral LiNa, where indeed multireference effects are present and CCSD(T) fails to correctly describe the bond cleavage.

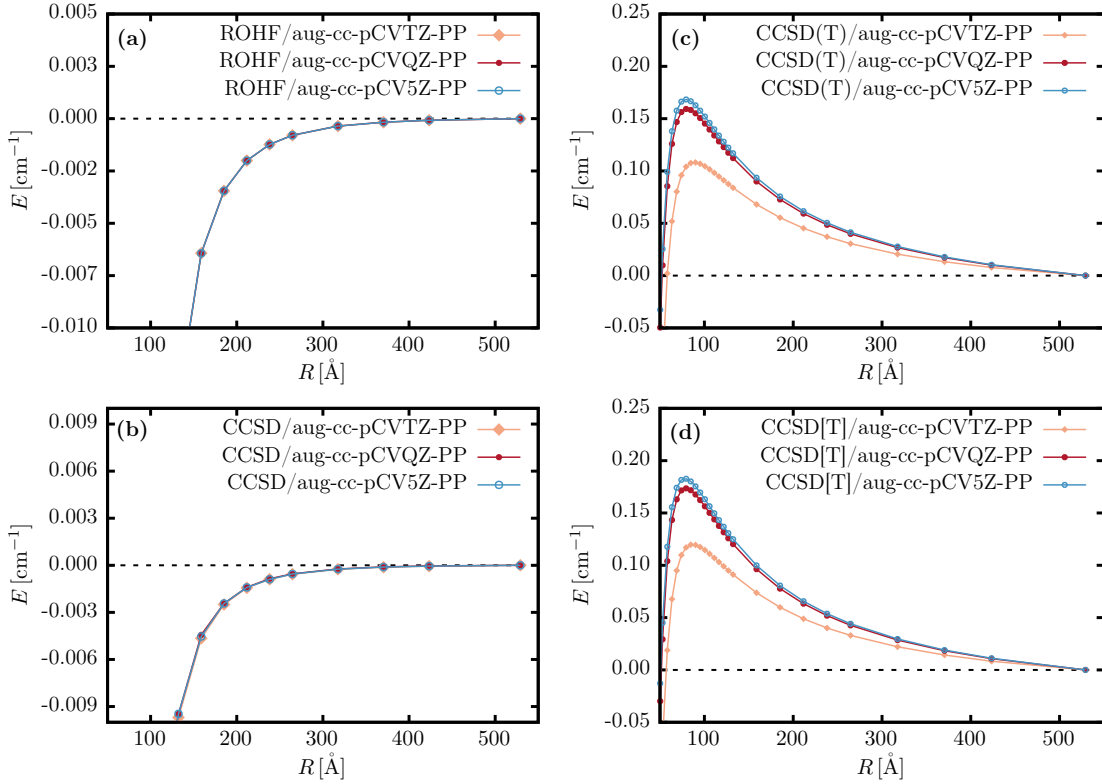


Figure 2. Overview of the long-range parts of the PECs of the Rb_2^+ ground state calculated at different levels of theory each using ECP28MDF. In (a) the reference energies (ROHF) are shown for the aug-cc-pCV n Z-PP basis sets. In (b) the coupled cluster energies with single and double excitations (CCSD) are shown. From Figs. (c) and (d) we obtain that including perturbative triples in the coupled cluster method either via (T) or [T] lead to unphysical humps in the long-range region. All energies were calculated with respect to the asymptote.

B. Higher excitations and iterative approximations

CCSD[T] and CCSD(T) are non-iterative approximations to CCSDT. To further investigate the origin of the long-range hump we also applied iterative approximations to full CCSDT: the CCSDT- n , with $n = 1b, 2, 3, 4$, methods^{41,42,61}. We used the ECP28MDF pseudopotential and the aug-cc-pCVTZ-PP basis set in these calculations.

As outlined in Sec. III these methods include contributions due to triples excitations conveyed via \hat{T}_3 into the solution of the coupled cluster equations. Here all approaches, except the CCSDT-4 method, avoid including any terms with N^8 scaling.

The resulting long-range PECs of these iterative

approximations to CCSDT are shown in Fig. 4 (a). Again, we obtain a hump for CCSDT-1b, CCSDT-2, CCSDT-3 at the same position ($\approx 100 \text{ \AA}$) and of the same magnitude ($\approx 0.1 \text{ cm}^{-1}$) as we have already seen for the non-iterative methods. Including more terms in the approximation scheme leads to a decrease in the size of the bump. However, only with the inclusion of the full Hamiltonian in the projection onto the excited triples manifold, i.e. for CCSDT-4, the artificial barrier disappears. But, as already mentioned this method is already as expensive as the full CCSDT calculation. The resulting long-range tails are presented in Fig. 4 (b) with both methods leading to the same shape in the asymptotic region.

This suggests the hypothesis that the

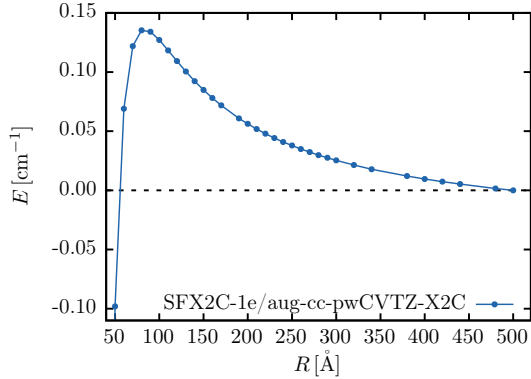


Figure 3. All electron SFX2C-1e calculation at ROHF-CCSD(T)/aug-cc-pwCVTZ-X2C level of theory. Here the *scECP* (ECP28MDF) is replaced by the X2C Hamiltonian thus correlating all electrons. Since we obtain the same long-range part as with ECP28MDF the hump is rather a general problem of the corresponding coupled cluster method than an artefact of the pseudopotential. The energies are calculated w.r.t. the last *ab-initio* point.

$\langle \Phi_0 | \hat{T}_3^\dagger \hat{f}_N \hat{T}_3 | \Phi_0 \rangle$ term, shared by all problematic methods (CCSD[T]/CCSD(T) as well), does not correctly account for interatomic interactions. In fact, this term only contains the interaction with the Hartree-Fock density of the other atom.

We obtain the same phenomenon if we perturbatively include even higher excitations such as CCSDT(Q). The corresponding result is shown in Fig. 5. The hump is smaller in size, as the contributions of connected quadruples are generally smaller than those of connected triples. Nevertheless, despite its smallness the artificial barrier completely spoils the long-range behavior of the potential, which is important for correct predictions on the scattering physics.

C. Symmetry breaking

In general X_2^+ – systems, with $X = \text{Li, Na, K, Rb, Cs}$, are characterized by the point group $D_{\infty h}$. This implies the asymptotical indistinguishability of $\text{Rb}^+ + \text{Rb}$ and $\text{Rb} + \text{Rb}^+$, which is also clear from a fundamental quantum mechanical point of view. The correct asymptotic behavior is given in terms of a

superposition of both limiting cases, i.e.

$$|X^2\Sigma_g^+\rangle = \frac{1}{\sqrt{2}} (|0,+\rangle + |+,0\rangle) \quad (13a)$$

$$|(1)^2\Sigma_u^+\rangle = \frac{1}{\sqrt{2}} (|0,+\rangle - |+,0\rangle). \quad (13b)$$

The zeroth-order description of the system is a mean-field approximation (Hartree-Fock), which involves the self-consistent-field (SCF) solution for the corresponding equations. This need for self-consistent solutions leads to different orbitals for Rb^+ and Rb and with that the solution of the separated fragments is at conflict with the symmetry requirement that the two cases $\text{Rb}^+ + \text{Rb}$ and vice versa are quantum-mechanical indistinguishable. All the orbitals of Rb and Rb^+ are a “compromise” of the neutral and ionic orbitals. The mean-field solution also defines the Fockian, the effective one-electron potential of the system. It plays an important role for defining perturbative approximations in the coupled-cluster equations. Here, rather than describing the correct superposition, it contains the compromise solution with half an electron on the right and half an electron on the left side, possibly explaining the repulsive long-range barrier.

If this is true, breaking the system’s symmetry should lead to a barrierless asymptotic behavior and thus size consistent mean-field solutions should be elements of the point group $C_{\infty v}$. Quantum mechanically speaking we project on one of the two limiting cases ($|0,+\rangle = \text{Rb} + \text{Rb}^+$ or vice versa $|+,0\rangle$). To test this hypothesis, we carried out CCSD, CCSD[T] and CCSD(T) computations using symmetry-broken ROHF orbitals. The resulting long-range tails of the PECs are given in Fig. 6. The results from Sec. IV A shown in Fig. 2 are given for comparison.

The results demonstrate that the long-range hump can be avoided by reducing the symmetry to $C_{\infty v}$. At short-range these symmetry-broken solutions collapse to the symmetric one. This is illustrated in more detail in the supplementary material. The findings suggest that the best model for the long-range region is based on the symmetry-broken solutions. So far the most promising approach is to use symmetry-broken (T) and (Q) corrections for the long-range tail and properly merge with symmetry-adapted solutions for smaller internuclear distances. With this all terms in the additivity scheme according to Eq. (2)

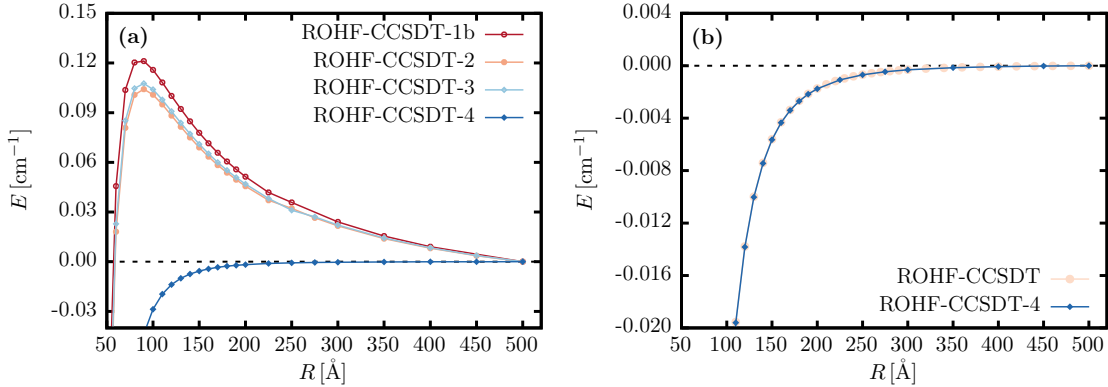


Figure 4. (a) Long-range part of the interaction energies using different iterative approximations to CCSDT. (b) Comparison of CCSDT-4 and full CCSDT interaction energies. All computations use a ECP28MDF pseudopotential, a aug-cc-pCVTZ-PP basis set, and an ROHF reference.

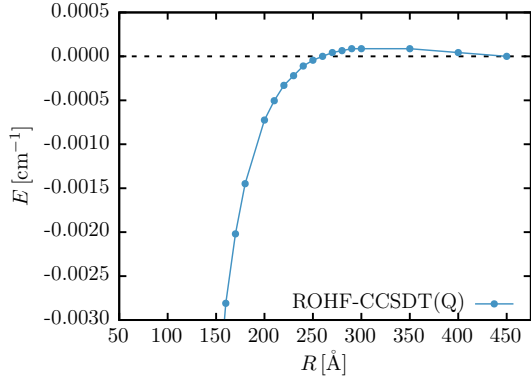


Figure 5. ROHF-CCSDT(Q) long-range part of the interaction energy w.r.t. the last *ab-initio* point calculated with the MRCC program suite using ECP28MDF/aug-cc-pwCVTZ-PP. The hump moved to the right compared to UCCSD(T) and the iterative approximations to CCSDT. It is smaller in size since (Q) corrections are in general smaller than (T) ones.

are well-defined paving the way for a highly accurate PEC. The details on this will be published in a subsequent study.

V. DISCUSSION

Our findings so far suggest that the physical origin of the artificial long-range humps is connected with the underlying mean-field character of our calculations and the way it enters coupled cluster approximations. To fully understand the problem and to reveal the source of error in approximative coupled cluster methods we have to go further into the theory and investigate the coupled cluster equations (3) in more detail.

A. Qualitative Analysis

The $E^{(5)}$ energy contribution is shown in Fig. 7 (a) with the area usually containing the artificial long-range barrier highlighted in gray. The inset demonstrate that in this region the fifth-order term is purely attractive. This finally explains our observations from Fig. 2 of Sec. IV A showing a slightly more pronounced long-range hump for [T] corrections compared to (T) ones. Furthermore, as shown in Fig. 7 (b), we can conclude that the pure fifth-order correction is not connected to the discussed problem.

However, a priori it is still not clear whether the nature of this phenomenon is due the approximation in the energy expression or due to the use of approx-

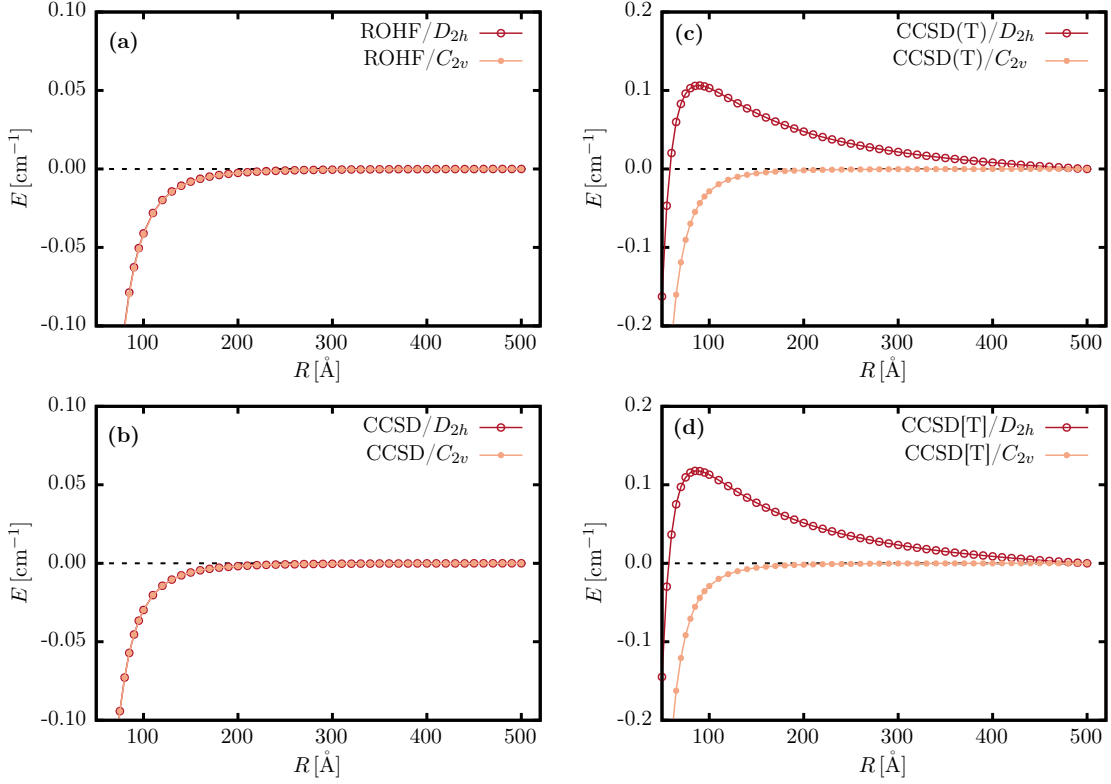


Figure 6. Comparison of the long-range parts using either symmetry-adapted (D_{2h}) or symmetry-broken (C_{2v}) ROHF orbitals. In (a) the reference (ROHF) interaction energies are given w.r.t. the asymptote. In (b) the CCSD results are depicted, while (c) and (d) corresponding to CCSD(T), respectively CCSD[T] interaction energies. All results were computed using ECP28MDF/aug-cc-pCVTZ-PP.

imate triples amplitudes. The latter can be tested rather systematically by using \hat{T}_3 amplitudes from CCSDT in Eq. (8). This will be investigated in the following.

B. Straightforward improvement of the triples correction

To understand the appearance of artificial humps in the CCSD(T) curves, we carried out calculations using a closely related formulation for the triples contribution based on analytic energy derivative formulation of CCSD.^{64,65} A CCSD Lagrangian^{56,66} with triple excitations treated as an “external” perturbation with a fictitious field strength χ is used

here

$$\mathcal{L}(\hat{T}_1, \hat{T}_2, \chi \hat{T}_3) = \langle 0 | (1 + \hat{\Lambda}_{\text{CCSD}}) \bar{H}[\chi] | 0 \rangle, \quad (14)$$

in which $\hat{\Lambda}_{\text{CCSD}} = \hat{\Lambda}_{1,\text{CCSD}} + \hat{\Lambda}_{2,\text{CCSD}}$ represents the CCSD Λ operator, and \hat{T}_3 contributes to \bar{H} , defined in Eq. (4), in the same way as in the CCSDT method. Given the exact \hat{T}_3 , a finite-field CCSD calculation defined as the left-hand side of Eq. (14) with $\chi = 1$ produces the exact CCSDT energy. This finite field CCSD calculation uses the CCSDT equation, but treats the triples as the perturbation. Hence the

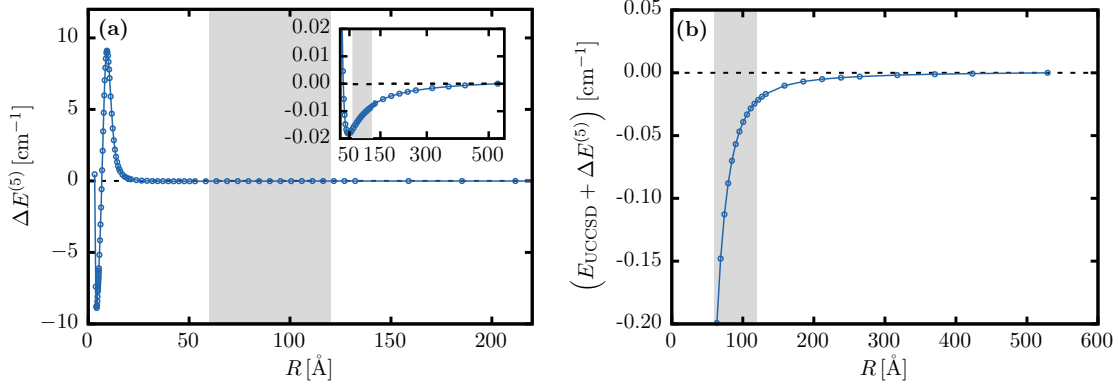


Figure 7. Visualization of the impact of the fifth-order perturbative triples correction as non-iterative approximation to CCSDT. The pure fifth-order energy term according to Eqs. (11) is given in (a) relative to the asymptote. Adding $\Delta E^{(5)}$ to the CCSD energy leads to the correct long-range behaviour as shown in (b). The areas highlighted in gray mark the position of the long-range hump, where the inset in (a) shows a zoom into this area.

CCSDT energy can be expanded in a Taylor series

$$\begin{aligned}
 E_{\text{CCSDT}} &= \mathcal{L}(\hat{T}_1, \hat{T}_2, \chi \hat{T}_3) \Big|_{\chi=1} \\
 &= \left[\mathcal{L} \Big|_{\chi=0} + \chi \frac{d\mathcal{L}}{d\chi} \Big|_{\chi=0} \right. \\
 &\quad \left. + \frac{1}{2} \chi^2 \frac{d^2\mathcal{L}}{d\chi^2} \Big|_{\chi=0} + \dots \right] \Big|_{\chi=1} \\
 &= \mathcal{L} \Big|_{\chi=0} + \frac{d\mathcal{L}}{d\chi} \Big|_{\chi=0} + \frac{1}{2} \frac{d^2\mathcal{L}}{d\chi^2} \Big|_{\chi=0} + \dots,
 \end{aligned} \tag{15}$$

with the unperturbed energy being the CCSD energy

$$\mathcal{L} \Big|_{\chi=0} = E_{\text{CCSD}} \tag{16}$$

and the first-order correction given by

$$\begin{aligned}
 \frac{d\mathcal{L}}{d\chi} \Big|_{\chi=0} &= \left\langle 0 \left| \hat{\Lambda}_{\text{CCSD}} \frac{\partial \hat{H}[\chi]}{\partial \chi} \right| 0 \right\rangle \Big|_{\chi=0} \\
 &= \langle 0 | \hat{\Lambda}_{\text{CCSD}} [\hat{H}, \hat{T}_3] | 0 \rangle.
 \end{aligned} \tag{17}$$

Eq. (17) offers a flexible framework for obtaining leading triples corrections to the CCSD energy. When the leading-order contribution to \hat{T}_3 is used, i.e. the triples amplitudes defined in Eq. (10), Eq. (17)

reduces to the CCSD(T)_{Λ} method originally derived within the equation-of-motion CC framework.⁴⁸⁻⁵⁰ Eq. (17) is also compatible with the use of improved \hat{T}_3 amplitudes obtained from iterative solutions of the CCSDT amplitude equations. This is particularly useful for the present purpose to understand whether the small humps in the CCSD(T) potential energy curves originate from the approximation in the energy expression or from the approximation of using leading-order \hat{T}_3 . A straightforward approach to improve \hat{T}_3 is to solve the CCSDT amplitude equations iteratively. Here we define $E_{\text{T}}[\text{CCSD(T)}_{\Lambda}\text{-}n]$ as the triples energy correction using Eq. (17) with $\hat{T}_{3,n}$ 'th obtained from the n 'th iteration of CCSDT equations with converged CCSD amplitudes adopted as the initial guess

$$E_{\text{T}}[\text{CCSD(T)}_{\Lambda}\text{-}n] = \langle 0 | \hat{\Lambda}_{\text{CCSD}} [\hat{H}, \hat{T}_{3,n}^{\text{th}}] | 0 \rangle. \tag{18}$$

The use of T_3 from a converged CCSDT calculation provides the first-order correction from the triples amplitudes to the CCSD energy

$$E_{\text{T}}[\text{CCSD(T)}_{\Lambda}\text{-conv}] = \langle 0 | \hat{\Lambda}_{\text{CCSD}} [\hat{H}, \hat{T}_{3,\text{CCSDT}}] | 0 \rangle. \tag{19}$$

Here “-conv” denotes the use of converged CCSDT \hat{T}_3 . Although it is obviously not practically useful, Eq. (19) defines the limit of the accuracy that can be obtained using Eq. (17).

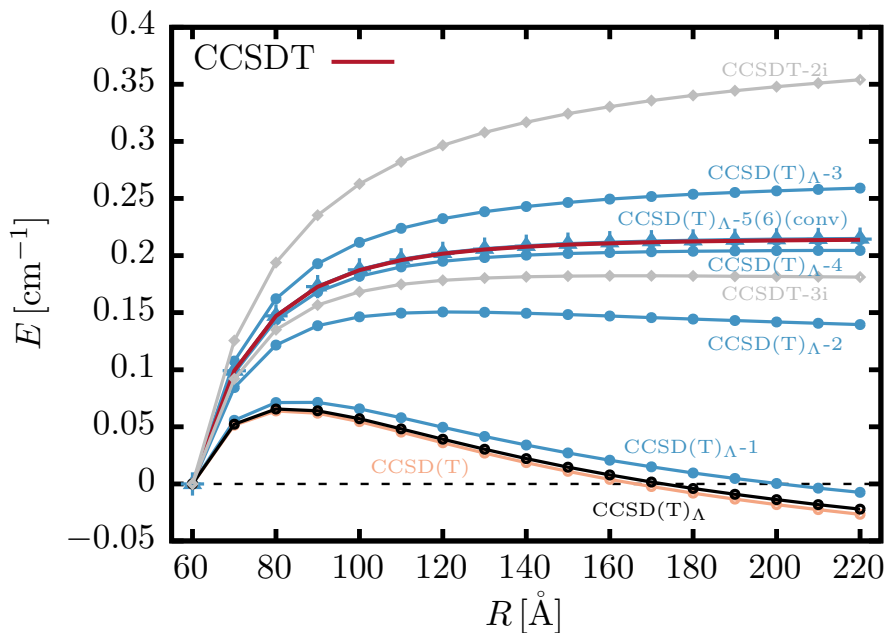


Figure 8. Comparison of potential energy curves of Rb_2^+ calculated with ECP28MDF/aug-cc-pwCVTZ-PP and different levels of the CCSD(T)_{Λ} - n method introduced in this work (see text for more details). The method refers to the use of \hat{T}_3 amplitudes obtained at the m 'th CCSDT iteration. CCSD(T)_{Λ} -conv denotes the use of converged triples amplitudes. CCSDT-2i(3i) is the CCSDT energy after the second (third) iteration. All PECs are plotted w.r.t. $R = 60 \text{ \AA}$.

The CCSD(T)_{Λ} - n methods are related to available methods for obtaining triples corrections,^{67–73} the most intimately to the CCSD(T-n) methods^{71–73} derived using CCSD Lagrangian, which also treats CCSD as the unperturbed state. The difference lies in that the schemes outlined so far refrain from performing an Møller-Plesset perturbation analysis and limit the consideration to the first derivative with respect to the triples amplitudes, whereas, the CCSD(T-n) derivation expands the Lagrangian order by order in terms of the fluctuation potential. Since the first iteration of CCSDT amplitude equations in CCSD(T)_{Λ} - n uses CCSD solutions as the initial guess and generates first-order \hat{T}_3 . Substituting this \hat{T}_3 into Eq. (17) gives a triples correction correct to second-order, i.e., CCSD(T)_{Λ} -1 appears to be equivalent to CCSD(T-2) . CCSD(T-4) contains contributions from higher order, i.e., the second term in Eq. (15), which is not considered in CCSD(T)_{Λ} - n . The CCSD(T-n) methods are more efficient, since no storage of T_3 is needed.

However, the CCSD(T)_{Λ} - n approaches may have the advantage that the use of convergence-acceleration techniques during iterative solutions of CCSDT equation such as direct inverse of iterative space (DIIS)⁷⁴ may smooth the convergence when the plain iterative solutions exhibit an oscillating behavior.

We have performed CCSD(T)_{Λ} - n , $n = 1 - 6$ and CCSD(T)_{Λ} - ∞ calculations for potential energy surfaces of Rb_2^+ using aug-cc-pwCVTZ basis set. As shown in Fig. 8, the CCSD(T)_{Λ} - n results systematically converge to the CCSD(T)_{Λ} - ∞ results, which is essentially indistinguishable from CCSDT results. The CCSD(T)_{Λ} -1 curve shows an artificial hump similar to the case of CCSD(T)_{Λ} . The hump is significantly reduced in the CCSD(T)_{Λ} -2 curve and is eliminated using methods with more than two iterations. These results clearly support that the artificial hump in the CCSD(T)_{Λ} curve originates from the approximation of \hat{T}_3 . This is also true for iterative approximations to CCSDT, i.e. CCSDT-n ($n = 1, 2, 3$)

since the equation for determining triples amplitudes approximately is formally similar to Eq. (10). The physical explanation behind this is based on the underlying mean-field approximation and the need to define self-consistent solutions leading to different orbitals for Rb^+ and Rb which has been already discussed in detail in Sec. IV C.

Note that the CCSD(T)_{Λ} -n energies converge more rapidly than CCSDT energies with respect to iterative solution of CCSDT amplitude equations, as also demonstrated in Fig. 8. The CCSD(T)_{Λ} -n triples correction is less sensitive to the quality of \hat{T}_3 , since it is only a small fraction of the total CCSDT energy. Finally, we note that, while the CCSD(T)_{Λ} -n methods have proven useful in the present context, the potential usefulness in calculations of chemical properties remains to be explored.

VI. CONCLUSION

This work shows that several standard coupled-cluster methods with noniterative or approximative iterative treatments of triple excitations can lead to unphysical potential energy curves for X_2^+ systems, $\text{X} \in \{\text{Li}, \text{Na}, \text{K}, \text{Rb}, \text{Cs}\}$, with a repulsive long range barrier. Although this effect is in the order $\mathcal{O}(10^{-1} \text{cm}^{-1})$ it would lead to severe problems when using the corresponding PECs for highly accurate studies in the context of ultracold chemistry. We unraveled the origin of this phenomenon by studying the ground state PEC of Rb_2^+ . It arises from the need to define self-consistent solutions which at the same time cannot be both consistent with the separated fragments (different orbitals for Rb^+ and Rb) and with the quantum mechanically imposed symmetry requirement (indistinguishable cases $\text{Rb}^+ + \text{Rb}$ and $\text{Rb} + \text{Rb}^+$). This problem lives on in the Fockian and affects the perturbative estimates of the \hat{T}_3 amplitudes, which finally lead to the wrong behavior of the PEC. This was demonstrated quantitatively by using a new “ CCSD(T)_{Λ} -n” scheme.

For the Rb_2^+ molecule we found that symmetry-broken CCSD(T) solutions lead to physically correct long-range PECs while symmetry-broken and non-broken CCSD curves virtually coincide in this region. From this we conclude that (T) corrections from symmetry- broken calculations can be used for

estimating the complete basis set limit of the long-range part of the PEC. In the same way we could proceed with (Q) corrections and smaller basis sets eventually defining a protocol for obtaining a highly accurate global PEC for the ground state of Rb_2^+ . This will be thoroughly investigated in a subsequent study.

SUPPLEMENTARY MATERIAL

See supplementary material for technical details on the independence of the long-range hump on possible sources of error, for the universality of the current problem for X_2^+ systems and for more details on symmetry breaking.

ACKNOWLEDGMENTS

J.S. and A.K. would like to acknowledge funding by IQST. The research of IQST is financially supported by the Ministry of Science, Research, and Arts Baden-Württemberg. The work at Johns Hopkins university has been supported by the National Science Foundation, under grant No. PHY-2011794.

DATA AVAILABILITY

The data that support the findings of this study are available within this article and its supplementary material.

REFERENCES

- ¹W. Ketterle, *Rev. Mod. Phys.* **74**, 1131 (2002).
- ²M. Schlagmüller, T. C. Liebisch, F. Engel, K. S. Kleinbach, F. Böttcher, U. Hermann, K. M. Westphal, A. Gaj, R. Löw, S. Hofferberth, T. Pfau, J. Pérez-Ríos, and C. H. Greene, *Phys. Rev. X* **6**, 031020 (2016).
- ³T. C. Liebisch, M. Schlagmüller, F. Engel, H. Nguyen, J. Balewski, G. Lochead, F. Böttcher, K. M. Westphal, K. S. Kleinbach, T. Schmid, A. Gaj, R. Löw, S. Hofferberth, T. Pfau, J. Pérez-Ríos, and C. H. Greene, *J. Phys. B* **49**, 182001 (2016).
- ⁴F. Böttcher, A. Gaj, K. M. Westphal, M. Schlagmüller, K. S. Kleinbach, R. Löw, T. C. Liebisch, T. Pfau, and S. Hofferberth, *Phys. Rev. A* **93**, 032512 (2016).

- ⁵M. Deiß, B. Drews, J. Hecker Denschlag, N. Bouloufa-Maafa, R. Vexiau, and O. Dulieu, *New J. Phys.* **17**, 065019 (2015).
- ⁶B. Drews, M. Deiß, K. Jachymski, Z. Idziaszek, and J. Hecker Denschlag, *Nature Commun.* **8**, 14854 (2017).
- ⁷B. Drews, M. Deiß, J. Wolf, E. Tiemann, and J. Hecker Denschlag, *Phys. Rev. A* **95**, 062507 (2017).
- ⁸M. Tomza, K. Jachymski, R. Gerritsma, A. Negretti, T. Calarco, Z. Idziaszek, and P. S. Julienne, *Rev. Mod. Phys.* **91**, 035001 (2019).
- ⁹R. Côté and A. Dalgarno, *Phys. Rev. A* **62**, 012709 (2000).
- ¹⁰Z. Idziaszek, T. Calarco, P. S. Julienne, and A. Simoni, *Phys. Rev. A* **79**, 010702 (2009).
- ¹¹T. Schmid, C. Veit, N. Zuber, R. Löw, T. Pfau, M. Tarana, and M. Tomza, *Phys. Rev. Lett.* **120**, 153401 (2018).
- ¹²K. Kleinbach, F. Engel, T. Dieterle, R. Löw, T. Pfau, and F. Meinert, *Phys. Rev. Lett.* **120**, 193401 (2018).
- ¹³F. Engel, T. Dieterle, T. Schmid, C. Tomschitz, C. Veit, N. Zuber, R. Löw, T. Pfau, and F. Meinert, *Phys. Rev. Lett.* **121**, 193401 (2018).
- ¹⁴S. H. Patil and K. T. Tang, *J. Chem. Phys.* **106**, 2298 (1997).
- ¹⁵K. Jachymski, M. Krych, P. S. Julienne, and Z. Idziaszek, *Phys. Rev. Lett.* **110**, 213202 (2013).
- ¹⁶K. Jachymski, M. Krych, P. S. Julienne, and Z. Idziaszek, *Phys. Rev. A* **90**, 042705 (2014).
- ¹⁷S. Magnier, S. Rousseau, A. Allouche, G. Hadinger, and M. Aubert-Frécon, *Chem. Phys.* **246**, 57 (1999).
- ¹⁸H. Berriche, *Int. J. Quant. Chem.* **113**, 2405 (2013).
- ¹⁹S. Magnier and M. Aubert-Frécon, *J. Quant. Spectrosc. Ra.* **78**, 217 (2003).
- ²⁰A. Jraj, A. Allouche, M. Korek, and M. Aubert-Frécon, *Chem. Phys.* **290**, 129 (2003).
- ²¹D. Feller, *J. Chem. Phys.* **98**, 7059 (1993).
- ²²T. Helgaker, W. Klopper, H. Koch, and J. Noga, *J. Chem. Phys.* **106**, 9639 (1997).
- ²³J. M. L. Martin and G. de Oliveira, *J. Chem. Phys.* **111**, 1843 (1999).
- ²⁴A. Tajti, P. G. Szalay, A. G. Császár, M. Kállay, J. Gauss, E. F. Valeev, B. A. Flowers, J. Vázquez, and J. F. Stanton, *J. Chem. Phys.* **121**, 11599 (2004).
- ²⁵M. S. Schuurman, S. R. Muir, W. D. Allen, and H. F. Schaefer III, *J. Chem. Phys.* **120**, 11586 (2004).
- ²⁶D. Feller, K. A. Peterson, and D. A. Dixon, *J. Chem. Phys.* **129**, 204105 (2008).
- ²⁷Y. J. Bomble, J. Vázquez, M. Kállay, C. Michauk, P. G. Szalay, A. G. Császár, J. Gauss, and J. F. Stanton, *J. Chem. Phys.* **125**, 064108 (2006).
- ²⁸I. S. Lim, P. Schwerdtfeger, B. Metz, and H. Stoll, *J. Chem. Phys.* **122**, 104103 (2005).
- ²⁹K. G. Dyall, *J. Chem. Phys.* **115**, 9136 (2001).
- ³⁰W. Liu and D. Peng, *J. Chem. Phys.* **131**, 1 (2009).
- ³¹K. Raghavachari, G. W. Trucks, J. A. Pople, and M. Head-Gordon, *Chem. Phys. Lett.* **157**, 479 (1989).
- ³²R. J. Bartlett, J. D. Watts, S. A. Kucharski, and J. Noga, *Chem. Phys. Lett.* **165**, 513 (1990).
- ³³C. Hampel, K. A. Peterson, and H.-J. Werner, *Chem. Phys. Lett.* **190**, 1 (1992).
- ³⁴J. D. Watts, J. Gauss, and R. J. Bartlett, *Chem. Phys. Lett.* **200**, 1 (1992).
- ³⁵J. Noga and R. J. Bartlett, *J. Chem. Phys.* **86**, 7041 (1987).
- ³⁶G. E. Scuseria and H. F. Schaefer III, *Chem. Phys. Lett.* **152**, 382 (1988).
- ³⁷Y. J. Bomble, J. F. Stanton, M. Kállay, and J. Gauss, *J. Chem. Phys.* **123**, 054101 (2005).
- ³⁸M. Kállay and J. Gauss, *J. Chem. Phys.* **123**, 214105 (2005).
- ³⁹M. Kállay and J. Gauss, *J. Chem. Phys.* **129**, 144101 (2008).
- ⁴⁰J. G. Hill and K. A. Peterson, *J. Chem. Phys.* **147**, 244106 (2017).
- ⁴¹Y. S. Lee, S. A. Kucharski, and R. J. Bartlett, *J. Chem. Phys.* **81**, 5906 (1984).
- ⁴²J. Noga, R. J. Bartlett, and M. Urban, *Chem. Phys. Lett.* **134**, 126 (1987).
- ⁴³H.-J. Werner, P. J. Knowles, G. Knizia, F. R. Manby, and M. Schütz, *WIREs Comput. Mol. Sci.* **2**, 242 (2012).
- ⁴⁴H.-J. Werner, P. J. Knowles, G. Knizia, F. R. Manby, M. Schütz, *et al.*, “Molpro, version 2018.2, a package of ab initio programs,” (2018), see <http://www.molpro.net>.
- ⁴⁵P. J. Knowles, C. Hampel, and H. J. Werner, *J. Chem. Phys.* **99**, 5219 (1993).
- ⁴⁶P. J. Knowles, C. Hampel, and H.-J. Werner, *J. Chem. Phys.* **112**, 3106 (2000).
- ⁴⁷J. D. Watts, J. Gauss, and R. J. Bartlett, *J. Chem. Phys.* **98**, 8718 (1993).
- ⁴⁸J. F. Stanton, *Chem. Phys. Lett.* **281**, 130 (1997).
- ⁴⁹T. D. Crawford and J. F. Stanton, *Int. J. Quantum Chem.* **70**, 601 (1998).
- ⁵⁰S. A. Kucharski and R. J. Bartlett, *J. Chem. Phys.* **108**, 5243 (1998).
- ⁵¹J. F. Stanton, J. Gauss, L. Cheng, M. E. Harding, D. A. Matthews, and P. G. Szalay, “CFour, Coupled-Cluster techniques for Computational Chemistry, a quantum-chemical program package,” With contributions from A.A. Auer, R.J. Bartlett, U. Benedikt, C. Berger, D.E. Bernholdt, S. Blaschke, Y. J. Bomble, S. Burger, O. Christiansen, D. Datta, F. Engel, R. Faber, J. Greiner, M. Heckert, O. Heun, M. Hilgenberg, C. Huber, T.-C. Jagau, D. Jonsson, J. Jusélius, T. Kirsch, K. Klein, G.M. KopperW.J. Lauderdale, F. Lipparini, T. Metzroth, L.A. Mück, D.P. O’Neill, T. Nottoli, D.R. Price, E. Prochnow, C. Puzzarini, K. Ruud, F. Schiffmann, W. Schwalbach, C. Simmons, S. Stopkowicz, A. Tajti, J. Vázquez, F. Wang, J.D. Watts and the integral packages MOLECULE (J. Almlöf and P.R. Taylor), PROPS (P.R. Taylor), ABACUS (T. Metzroth, H.J. Aa. Jensen, P. Jørgensen, and J. Olsen), and ECP routines by A. V. Mitin and C. van Wüllen. For the current version, see <http://www.cfour.de>.
- ⁵²D. A. Matthews, L. Cheng, M. E. Harding, F. Lipparini, S. Stopkowicz, T.-C. Jagau, P. G. Szalay, J. Gauss, and J. F. Stanton, *J. Chem. Phys.* **152**, 214108 (2020).
- ⁵³L. Cheng and J. Gauss, *J. Chem. Phys.* **135**, 084114 (2011).
- ⁵⁴M. Kállay, P. R. Nagy, Z. Rolik, D. Mester, G. S. J. Csontos, J. Csóka, B. P. Szabó, L. Gyevi-Nagy, I. Ladjászki, L. Szegegy, B. Ladóczki, K. Petrov, M. Farkas, P. D. Mezei, and B. Hégyely, “MRCC, a quantum chemical program suite,” (2019), see www.mrcc.hu.
- ⁵⁵M. Kállay and P. R. Surján, *J. Chem. Phys.* **115**, 2945 (2001).
- ⁵⁶J. Arponen, *Ann. Phys.* **151**, 311 (1983).

- ⁵⁷M. Urban, J. Noga, S. J. Cole, and R. J. Bartlett, *J. Chem. Phys.* **83**, 4041 (1985).
- ⁵⁸J. F. Stanton, W. N. Lipscomb, D. H. Mager, and R. J. Bartlett, *J. Chem. Phys.* **90**, 1077–1082 (1989).
- ⁵⁹Y. S. Lee, S. A. Kucharski, and R. J. Bartlett, *J. Chem. Phys.* **81**, 5906 (1984).
- ⁶⁰J. Noga, R. Bartlett, and M. Urban, *Chem. Phys. Lett.* **134**, 126 (1987).
- ⁶¹Y. He, Z. He, and D. Cremer, *Theor. Chem. Acc.* **105**, 182 (2001).
- ⁶²M. Urban, I. Cernusak, V. Kellö, and J. Noga, *Electron correlation in atoms and molecules. Methods in computational chemistry*, Vol. 1 (S. Wilson (ed), New York, 1987) p. 117.
- ⁶³D. A. Fedorov, A. Derevianko, and S. A. Varganov, *J. Chem. Phys.* **140**, 184315 (2014).
- ⁶⁴L. Adamowicz and R. J. Bartlett, *Int. J. Quantum Chem. Symp.* **26**, 245 (1984).
- ⁶⁵A. C. Scheiner, G. E. Scuseria, J. E. Rice, T. J. Lee, and H. F. Schaefer III, *J. Chem. Phys.* **87**, 5361 (1987).
- ⁶⁶T. Helgaker and P. Jørgensen, *Adv. Quant. Chem.* **19**, 188 (1988).
- ⁶⁷S. Hirata, M. Nooijen, I. Grabowski, and R. J. Bartlett, *J. Chem. Phys.* **114**, 3919 (2001).
- ⁶⁸M. W. Włoch and P. Piecuch, *J. Chem. Phys.* **123**, 224105 (2005).
- ⁶⁹M. W. Włoch, M. D. Lodriguito, P. Piecuch, and J. R. Gour, *Mol. Phys.* **104**, 2149 (2006).
- ⁷⁰M. W. Włoch, M. D. Lodriguito, P. Piecuch, and J. R. Gour, *Mol. Phys.* **104**, 2991 (2006).
- ⁷¹J. J. Eriksen, K. Kristensen, T. Kjærgaard, P. Jørgensen, and J. Gauss, *J. Chem. Phys.* **140**, 064108 (2014).
- ⁷²J. J. Eriksen, P. Jørgensen, J. Olsen, and J. Gauss, *J. Chem. Phys.* **140**, 174114 (2014).
- ⁷³J. J. Eriksen, D. A. Matthews, P. Jørgensen, and J. Gauss, *J. Chem. Phys.* **143**, 041101 (2015).
- ⁷⁴P. Pulay, *Chem. Phys. Lett.* **73**, 393 (1980).